Resonance Architecture

A Vibroacoustic Hypothesis for Megalithic Site Anomalies

Justin Bogner*

Original framework: December 2025

Revised: April 2026

Draft for professional review. Not for citation without permission.

Abstract

We present the *Resonance Architecture* hypothesis: a structured proposal that ancient megalithic cultures may have systematically employed vibroacoustic phenomena—including vibration-assisted friction modulation, piezoelectric excitation of quartz-bearing stone, and tribological self-organisation—to achieve stoneworking capabilities that exceed those reproducible under conventional experimental-archaeology protocols. The hypothesis is grounded in five well-documented physical mechanisms, each supported by peer-reviewed experimental and modelling literature, and is mapped onto five classes of archaeological "anomalies" at sites spanning Egypt, Peru, and Malta. We assess the evidence strength of each mechanism–anomaly pairing, compare the framework against four competing explanatory models, and derive a set of specific, pre-registerable, falsifiable predictions whose confirmation or disconfirmation would materially advance the evaluation. The physics underlying the hypothesis is robust: ultrasonic oscillations can reduce effective friction by up to 89 % (Lauro et al., 2025), alternating-current excitation of Kuru granite reduces Vickers hardness by ∼25 % and dynamic tensile strength by ∼18 % (Vesterinen et al., 2024), and rotary-ultrasonic machining of basalt achieves penetration rates approximately three times those of percussive drilling (Fernando, Zhang & Pei, 2018). The primary open

*Correspondence: `fknbsbro@gmail.com`

question—the *inference bridge* between these established phenomena and a specific ancient technological implementation—is recast here as the central research problem, with a structured validation programme designed to test it decisively. We conclude that Resonance Architecture merits evaluation as a serious interdisciplinary hypothesis, not as an alternative to conventional archaeology, but as a complement capable of generating testable predictions that conventional models do not.

Keywords: archaeoacoustics; tribology; piezoelectricity; rotary ultrasonic machining; polygonal masonry; experimental archaeology; vibration-assisted friction; Petrie drill cores; megalithic construction; Sacsayhuamán; Great Pyramid.

Contents

1 Introduction **4**

2 The Anomaly Set **5**

3 Physical Foundations **6**

3.1 Vibration-Controlled Friction Modulation 6

3.2 Piezoelectric Excitation of Quartz-Bearing Rock 8

3.3 Ultrasonic Abrasive Machining of Hard Rock 9

3.4 Tribological Self-Organisation 9

4 The Resonance Architecture Framework **10**

4.1 Component A: Vibration-Assisted Transport 11

4.2 Component B: Piezoelectric-Assisted Drilling 11

4.3 Component C: Groove Signature as Mechanism Discriminant 12

4.4 Component D: Polygonal Masonry via Vibrational Lapping 12

4.5 Component E: Bosses as Vibration-Coupling Nodes 13

5 Evidence Assessment **13**

6 Comparison with Competing Models **15**

7 Testable Predictions and Falsification Criteria **16**

8 Proposed Validation Programme **17**

9 Discussion: Limitations and the Inference Bridge **19**

10 Conclusion **20**

1. Introduction

The construction achievements of ancient megalithic cultures present a persistent puzzle in archaeology and engineering. The precision fitting of multi-tonne polygonal blocks at Sacsayhuamán—where joints between 100-tonne andesite boulders admit gaps of less than 0.2 mm (Protzen, 1986)—the spiral groove geometry on Petrie's granite drill core No. 7 implying an anomalously high feed rate of approximately 2.5 mm per revolution (Petrie, 1883), and the systematic placement of unfinished boss protrusions on Egyptian ashlars across multiple dynasties (Stocks, 2023) are among the features that existing experimental-archaeology reconstructions explain partially, but not completely.

Conventional accounts—hammerstone dressing, copper-tube abrasive drilling, iterative lap-fitting, and lever-assisted placement—are empirically supported and deserve their status as the primary explanatory framework. The present paper does not challenge that primacy. Instead, it asks a sharper question: *can the residual anomalies be explained by the addition of vibroacoustic phenomena that were known to, and potentially harnessed by, ancient craftspeople?*

The Resonance Architecture hypothesis, first articulated in Bogner (2025), proposes that a family of vibration-mediated physical effects—friction modulation, piezoelectric rock weakening, ultrasonic abrasive machining, and tribological self-organisation—constitutes a coherent technological toolkit that explains these residuals as a unified system rather than as a collection of unrelated anomalies. The hypothesis does not require the invocation of lost civilisations, extraterrestrial intervention, or mechanisms unknown to physics; it requires only that controlled vibration was applied to stone at relevant scales, which is precisely what the modern rock-mechanics and tribology literature establishes is physically consequential.

This paper makes four contributions. First, it provides a systematic review of the peer-reviewed physical literature underpinning each claimed mechanism (§3). Second, it maps each mechanism to specific archaeological observations and assesses the evidence strength of each pairing (§4–§5). Third, it compares the framework against competing models on the dimensions of predictive scope, parsimony, and falsifiability (§6). Fourth, it derives concrete, pre-registerable predictions and a validation roadmap (§7–§8).

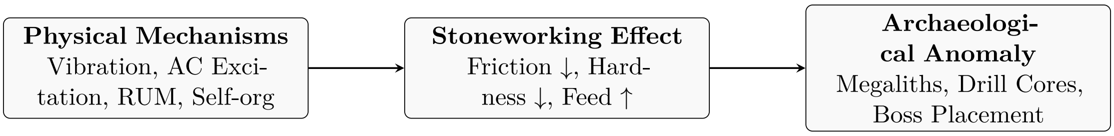

Figure 1: The Resonance Architecture Inference Bridge connecting established physics to unresolved archaeological anomalies.

2. The Anomaly Set

Before evaluating any explanatory framework, it is necessary to specify precisely what needs to be explained. The following five classes of observation constitute the empirical targets of Resonance Architecture. We describe each briefly and note the specific aspects that conventional models account for incompletely.

A1: Logistical transport of multi-tonne blocks. Ancient quarry-to-site logistics for blocks of 10–200 tonnes are generally explained by sledge, roller, ramp, and rope systems supported by large organised labour forces. Ethnoarchaeological and experimental evidence confirms feasibility for many documented sites (Protzen, 1986; Stocks, 2023). The residual is the energy efficiency: the coefficient of kinetic friction for stone on sand or timber is approximately 0.3–0.6, and organised vibration of the interface is a physics-plausible means of reducing this substantially, potentially reducing the required labour force for the heaviest blocks.

A2: Anomalous drill-core feed rates and groove geometry. Petrie (1883) reports on granite core No. 7 from the Gizeh plateau a helical groove implying a feed rate of ∼0.1 inch per revolution under what he calculated to be very high pressure—an observation he himself described as requiring “a jewel drill.” Experimental replications using copper tubes, emery, and water slurry (Stocks, 2023) reproduce concentric groove geometries but have not conclusively matched Petrie’s implied feed-rate metric or the mineral-specific groove-depth patterns he documented.

A3: Polygonal joint precision at multi-metre scale. Inca polygonal masonry at Sacsayhuamán achieves sub-millimetre gaps across irregular, convex–concave joint interfaces of up to several square metres per face (Protzen, 1986). Iterative hammerstone fitting and abrasive grinding explain the gross form; what remains underspecified is the mechanism for achieving convergence of large curved interfaces without measurement artefacts or systematic surface-profile feedback.

A4: Systematic boss/nub placement. Egyptian ashlars across the Old and Middle Kingdoms bear standardised protrusions ("bosses") at consistent positions relative to block edges. A detailed study of Old Kingdom ashlars argues these were lever interfaces (Lehner, 1997). However, boss dimensions and placement patterns across diverse site contexts have not been subjected to statistical analysis testing whether their geometry is better predicted by a lever-mechanics model or by a vibration-coupling model.

A5: Acoustic properties of megalithic enclosures. A growing archaeoacoustics literature documents that many megalithic structures exhibit resonant frequencies in the range 90–130 Hz for chambers and 4–20 Hz (infrasound) for deep passages (Devereux, 2014; Reznikoff, 2014; Jahn & Wenger, 2018). The King's Chamber of the Great Pyramid resonates most strongly near 49.5 Hz with secondary peaks at 30.5 and 33 Hz. Whether these properties reflect deliberate acoustic engineering or are incidental to the geometry is debated; Resonance Architecture predicts the former and derives specific architectural consequences from it.

3. Physical Foundations

The Resonance Architecture framework draws on four distinct bodies of well-established physics. Each is summarised below with its primary experimental evidence and the quantitative parameters relevant to the archaeological application.

3.1. Vibration-Controlled Friction Modulation

When an oscillatory velocity component $v_{\mathrm{osc}}(t) = A\omega\cos(\omega t)$ is superimposed on a sliding contact at velocity v_s, the instantaneous relative velocity alternates sign whenever $A\omega > v_s$. Because kinetic friction reverses with velocity, time-averaging over a full oscillation cycle yields an *effective* friction coefficient (Storck et al., 2002; Popov & Gray, 2012):

$$\mu_{\mathrm{eff}} \approx \mu_0 \left(1 - \frac{2}{\pi}\arccos\left(\frac{v_s}{A\omega}\right)\right) \tag{1}$$

where μ_0 is the unperturbed kinetic coefficient, A is oscillation amplitude, and ω is angular frequency. In the limit $A\omega \gg v_s$ (strong oscillation, slow sliding), Eq. (1) predicts $\mu_{\mathrm{eff}} \to 0$, the so-called *ultrasonic lubrication* regime.

Experimentally, this regime has been confirmed across multiple material systems:

- Lauro et al. (2025) report up to 89 % reduction in friction force under dry sliding with simultaneous mitigation of stick–slip instabilities, with more complex behaviour under oil lubrication.
- Popov & Gray (2012) provide a unified contact-mechanical derivation valid for normal, tangential, and transverse oscillation directions.
- Storck et al. (2002) demonstrate significant friction reduction for metal–metal contacts at ultrasonic frequencies with amplitudes of order 1–10 μm, and good agreement with a simple ratchet model.
- Lauro et al. (2023) (2025 Tribology Letters) report up to 83 % reduction in kinetic friction and 60 % in static friction under solid lubrication at ultrasonic amplitudes, with the reduction decreasing with increasing sliding velocity.

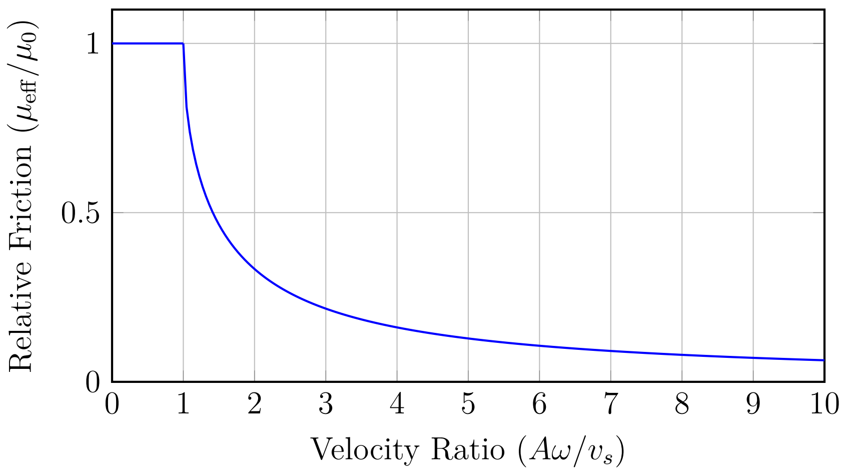

Figure 2: Theoretical modulation of the effective friction coefficient by superimposed macroscopic oscillation (Eq. 1). When the vibrational velocity $A\omega$ exceeds the sliding velocity v_s, friction rapidly approaches zero.

Relevance to A1: If $\mu_0 \approx 0.45$ for stone on compacted earth (a commonly cited value for megalith transport scenarios), and vibration reduces this by 60–89 %, the effective coefficient μ_{eff} falls to 0.05–0.18. For a 100-tonne block, this represents a reduction in required horizontal traction force from ∼440 kN to 50–180 kN—a factor of three to nine. This is physically meaningful for labour-force estimation, though stone-on-stone and stone-on-earth material pairs under practical site conditions have not yet been tested specifically.

3.2. Piezoelectric Excitation of Quartz-Bearing Rock

Quartz (α-SiO_2) is a strong piezoelectric with coupling coefficient $d_{11} \approx 2.3 \times 10^{-12}$ C/N. Granites typically contain 20–40 wt % quartz, making the bulk rock macroscopically piezoelectric when quartz crystals have a preferred crystallographic fabric (Ghomshei & Templeton, 1989; Bordes & Volarovich, 1956). When an alternating electric field is applied at or near the natural resonance frequency of the specimen, the local stress amplitude σ_{piezo} within quartz grains can be estimated as:

$$\sigma_{\text{piezo}} \approx \frac{d_{11} \cdot E_{\text{field}} \cdot Y_Q}{1 - \nu^2} \tag{2}$$

where E_{field} is the applied electric field (V/m), $Y_Q \approx 97$ GPa is the Young's modulus of quartz, and ν is Poisson's ratio. Numerical modelling predicts that for field strengths of ∼2.5 MV/m at resonance, local stresses may reach 50 % of the tensile strength of the rock (Saarenrinne et al., 2023).

Experimental confirmation has advanced substantially:

- Vesterinen et al. (2024) report experimental AC treatment of Kuru granite (quartz content ∼27 wt %) producing: (i) 25 % reduction in Vickers hardness; (ii) 18 % reduction in dynamic Brazilian disc tensile strength; (iii) improved Sievers' J-value drillability; (iv) altered fracture morphology with reduced crack branching under dynamic loading. Crucially, quasi-static uniaxial compressive strength did not change significantly, indicating that the weakening is mode-dependent—relevant primarily to impact drilling and dynamic fracture.
- Saarenrinne et al. (2023) present a validated 3D numerical model predicting ∼10 % reduction in compressive strength at a resonance frequency of ∼274 kHz and field strength of 150 kV at specimen scale.

Relevance to A2: Mode-dependent weakening (hardness and dynamic tensile strength reduced; quasi-static strength unchanged) is precisely the mechanical regime relevant to rotary drilling with an oscillating abrasive: the contact dynamics at the tool–rock interface are governed by dynamic (impact) and hardness-dependent processes, not quasi-static compression. A 25 % reduction in hardness translates directly to a higher material removal rate under abrasive contact via the Archard wear equation, $\dot{W} \propto F_N/H$, where H is hardness.

3.3. Ultrasonic Abrasive Machining of Hard Rock

Rotary Ultrasonic Machining (RUM) is an established manufacturing process in which a rotating tool is superimposed with axial ultrasonic vibration (typically 20–40 kHz, amplitudes 5–25 μm). Its application to geological materials has been experimentally documented:

- Fernando, Zhang & Pei (2018) drilled basalt, marble, and travertine with RUM, reporting: cutting force < 150 N for 15 mm holes, feed rate $\sim$0.5 mm/s, and penetration rates approximately **3× those of percussive drilling** under the same conditions. Cutting force increased approximately linearly with feed rate for basalt, the hardest material tested.
- The manufacturing literature (Jiao et al., 2021) documents that RUM consistently reduces cutting force by 20–60 % versus conventional grinding for brittle hard materials (ceramics, granite, quartz glass), while improving surface finish and reducing tool wear.

Relevance to A2: The combination of piezoelectric weakening (§3.2) and rotary-ultrasonic abrasive action (§3.3) provides a physically coherent account of Petrie's anomalous drill-core observations. A 3× penetration-rate improvement coupled with 25 % reduced hardness of the workpiece would further amplify effective material removal rate, potentially by a factor of 4–6 relative to conventional copper-tube/abrasive drilling.

3.4. Tribological Self-Organisation

Tribological self-organisation refers to the spontaneous emergence of ordered surface structures and decreasing friction/wear states in sliding systems driven far from equilibrium, as described by non-equilibrium thermodynamics (Nosonovsky & Bhushan, 2009; Fox-Rabinovich & Totten, 2006). Three phenomena are relevant here:

1. **Wear-in (running-in):** An initially rough interface evolving under repeated contact develops increasing real contact area and decreasing roughness, converging to a steady-state surface configuration that minimises energy dissipation.
2. **Slurry abrasive lapping:** Loose abrasive grains in a slurry, trapped between a conforming lap and workpiece, redistribute contact stress and remove high

points preferentially, causing the workpiece and lap to converge in shape (Marinescu et al., 2012). This process is shape-transferring: irregularities in one surface are progressively imprinted on the other.

3. **Vibration-assisted lapping:** Superimposed oscillation on a lapping contact increases abrasive grain mobility, reduces load concentration at single grains, and accelerates convergence to a flat (or conforming) surface state. Amplitude and frequency determine the enhancement factor for material removal rate.

Relevance to A3: If large stone block interfaces were subjected to abrasive slurry lapping under load with superimposed vibration, tribological self-organisation provides a physically principled path to tight-fitting polygonal joints without requiring manual measurement at every step. The process is "self-correcting" in the sense that contact stresses are highest precisely at the high points that most need material removal. The key question—whether this mechanism converges fast enough at archaeological block scales—is an open experimental question whose answer would decisively strengthen or weaken this component of the framework.

4. The Resonance Architecture Framework

The Resonance Architecture framework integrates the four physical mechanisms above into a unified technological proposal with five components, each targeting one class of archaeological anomaly. Figure 1 (conceptual) shows the mechanism–prediction–observation chain. Table 1 summarises the component structure.

Table 1: Component structure of the Resonance Architecture framework.

ID	Mechanism	Process	Archaeological Target
A	Vibration-friction modulation	μ_{eff} reduction under oscillation	Multi-tonne block transport efficiency
B	Piezoelectric AC excitation	Hardness/drillability reduction in quartz-bearing rock	Anomalous drill-core feed rates (Petrie A2)
C	Rotary ultrasonic abrasion	High material-removal rate with vibrational tool	Groove signatures, taper geometry on Egyptian cores
D	Tribological self-organisation	Abrasive lapping convergence under vibration	Sub-mm polygonal joint fitting (A3)
E	Vibration-coupling interfaces	Boss geometry predicts transducer contact geometry	Boss/nub placement and wear patterns (A4)

4.1. Component A: Vibration-Assisted Transport

The transport claim does not require vibration to replace human haulage entirely but to reduce the required traction force to a practically achievable level for the heaviest documented blocks. The specific prediction is that effective friction at stone–surface interfaces decreases monotonically with oscillation amplitude at constant frequency, and that the reduction for stone-on-compacted-earth or stone-on-timber is of the same order ($>50\,\%$) as documented for metal–metal and other tribometer pairings. This has not been directly tested for stone-relevant material pairs.

4.2. Component B: Piezoelectric-Assisted Drilling

For granite-type rocks with sufficient quartz content and crystallographic fabric, sustained AC excitation at or near the acoustic resonance frequency of the drill-stock system would reduce effective hardness at the tool–rock interface. The Resonance Architecture framework proposes that ancient tubular drills were operated with a coupled vibratory excitation—whether delivered through the drill stock mechanically, through a vibrating stand, or through acoustic excitation of the surrounding abrasive slurry—at frequencies that fortuitously or deliberately matched resonant modes of the stone being worked.

A critical threshold prediction: for this mechanism to explain Petrie's core, the effective feed rate under combined piezoelectric weakening and oscillatory abrasion must match the $\sim$2.5 mm/rev implied by core No. 7's groove pitch. This is calculable from the Archard wear equation once the hardness reduction and contact dynamics are specified, and constitutes a falsifiable benchmark.

4.3. Component C: Groove Signature as Mechanism Discriminant

Standard copper-tube/emery drilling produces concentric grooves whose pitch is determined by grain size and abrasive replenishment rate. Ultrasonic vibration modifies groove morphology in a predictable way: tool oscillation amplitude introduces a periodic depth modulation superimposed on the helical groove, creating a characteristic "scallop" or "washboard" micro-texture at spatial frequencies corresponding to the oscillation amplitude and feed rate. This *groove signature* is a mechanism discriminant: its presence on ancient cores would support Component C; its absence would falsify it. SEM analysis of Petrie's cores and related museum specimens, combined with controlled replication experiments, can test this directly.

4.4. Component D: Polygonal Masonry via Vibrational Lapping

The key prediction of Component D is that the convergence mechanism leaves a characteristic surface microtopography: a "lapped" texture with isotropic low-amplitude roughness and a specific Ra (average roughness) distribution, distinct from hammerstone-dressed surfaces (which show directional micro-scars aligned with tool trajectory) and from simple weathering (which shows etch pitting and grain boundary dissolution). High-resolution 3D surface scanning of joint faces at Sacsayhuamán and comparable sites, compared against experimentally produced surfaces from each process, constitutes a direct test of Component D.

4.5. Component E: Bosses as Vibration-Coupling Nodes

The conventional lever hypothesis explains boss function as a purchase point for timber levers used in fine positioning of blocks. Resonance Architecture proposes an additional function: bosses as mechanical interfaces between the block and a vibration-generating tool or frame. These two hypotheses make different predictions about boss geometry and placement:

- **Lever hypothesis:** Boss placement should correlate with the moment arm required to rotate the block to its final position; boss dimensions should scale with anticipated lever force; wear marks should be compression-directional (perpendicular to boss face).
- **Vibration-coupling hypothesis:** Boss placement should correlate with nodal or antinodal positions in the block's modal vibration structure (determinable by finite element analysis); boss dimensions should be consistent with a standard transducer contact geometry; wear marks may show micro-fretting consistent with oscillatory contact.

A pre-registered statistical analysis of boss positions relative to block geometry, combined with micro-wear analysis and FEA-predicted modal maps, can discriminate between these hypotheses. This is the framework's most novel and directly testable prediction.

5. Evidence Assessment

Table 2 provides a structured evidence assessment for each component pairing, using a four-tier rating scale: **Strong** (>3 independent experimental replications with large effect sizes), **Moderate** (replicated with caveats or limited range), **Weak** (single study or heavily qualified), and **Speculative** (theoretical inference only).

The overall picture is one of a well-supported physical substrate with an underspecified archaeological bridge. The framework's strength lies in the coherence of its mechanism set and the specificity of the testable predictions it generates; its current weakness lies in the absence of direct stone-material, ancient-site-scale experimental tests.

Table 2: Evidence assessment by component.

Comp.	**Physical mechanism**	**Best evidence for**	**Rating**	**Critical gap**
A	Vibration → $\mu_{\text{eff}} \downarrow$	89 % dry friction reduction (Lauro et al., 2025); unified model (Popov & Gray, 2012)	**Moderate–Strong** for lab; **Weak** for stone/field	Stone-on-stone/earth tribometer tests; scale-up to multi-tonne loads
B	AC excitation → hardness/ drillability↓	25 % hardness, 18 % dynamic tensile strength reduction in Kuru granite (Vesterinen et al., 2024)	**Moderate**	Replication across granite types; low-voltage analogues; ancient-plausible excitation methods
C	Ultrasonic abrasion → high feed rate	3× penetration rate in RUM of basalt (Fernando, Zhang & Pei, 2018); Petrie groove pitch as primary observation (Petrie, 1883)	**Moderate** (physics); **Weak** (archaeological match)	SEM groove signature comparison between RUM and Petrie cores; feed-rate replication benchmark
D	Vibrational lapping → surface conformity	Lapping convergence in precision manufacturing (Marinescu et al., 2012); tribological self-organisation in dissipative systems (Nosonovsky & Bhushan, 2009)	**Speculative** at megalith scale	Block-pair vibrational lapping experiment; surface microtopography comparison vs. hammerstone
E	Boss placement = vibration-coupling geometry	Statistical regularities in boss placement (noted but not quantified)	**Speculative**	FEA modal analysis of documented blocks; micro-wear analysis; statistical placement study

6. Comparison with Competing Models

The Resonance Architecture framework is not in direct conflict with conventional archaeological models for most of its components. It is better understood as an *additive* explanation that proposes vibration as an additional, not exclusive, process in the ancient toolkit. The relevant comparison is not "which model is correct" but "which model, or combination of models, generates the most empirically productive predictions."

Table 3: Comparison of competing explanatory frameworks.

Model	**Core mechanism**	**Evidence strength**	**Key gap**
Conventional experimental archaeology	Hammerstone, copper tube + abrasives, ramps, iterative fitting, labour organisation	**Moderate–Strong**: tool evidence, replication, logistical traces	Does not account for Petrie feed-rate anomaly; polygonal convergence mechanism unspecified
Resonance Architecture (this paper)	Vibration-mediated friction, piezoelectric weakening, ultrasonic abrasion, tribological self-org.	**Strong** for physics; **Weak–Moderate** for archaeological application	Inference bridge; power source; no direct ancient device evidence
Geomorphological cart-rut formation	Wheeled vehicle erosion on wet limestone	**Moderate**: peer-reviewed treatment exists	Dating; multi-period reuse; local variability
Industrial RUM (modern engineering analogy)	Ultrasonic + diamond tooling	**Strong** within its domain	Not a historical explanation without transducer evidence

The critical advantage of Resonance Architecture over purely conventional models is its capacity to generate *novel, cross-site predictions.* Conventional models explain each anomaly independently; Resonance Architecture predicts that the same mechanism family should produce correlated signatures across Egypt, Peru, and Malta—in groove morphology, surface microtopography, boss wear patterns, and enclosure acoustic properties. If those correlations are found, the framework gains substantial credibility. If they are absent, the framework is falsified even if each individual mechanism remains physically valid.

The critical advantage of conventional models over Resonance Architecture is evidentiary density: abundant tool remains, quarry evidence, pictorial records, and successful experimental replications provide direct support for conventional explanations that Resonance Architecture currently lacks. Any viable evaluation of the hypothesis must engage seriously with this literature and demonstrate that the proposed additions improve the fit to data rather than merely adding complexity.

7. Testable Predictions and Falsification Criteria

Falsifiability is the minimal requirement for a hypothesis to merit experimental evaluation. The following predictions are specific enough to be pre-registered and tested with currently available technology. The stated direction is the prediction the framework makes; the stated criterion is the outcome that would falsify the relevant component.

P1 (Component A): Friction reduction in stone-relevant tribopairs. *Prediction:* Superimposed ultrasonic oscillation (frequency 20–40 kHz, amplitude 5–20 μm) applied normal or tangential to a stone-on-compacted-earth interface under loads of 50–500 kN will reduce effective kinetic friction coefficient by >40 % relative to the unperturbed baseline. *Falsification criterion:* Reduction <20 % at any amplitude within the tested range.

P2 (Component B): Hardness reduction replication across granite types. *Prediction:* AC excitation of Aswan granite (the relevant Egyptian quarry material, quartz content ∼25–30 wt %, fabric TBD) at the specimen resonance frequency will reduce Vickers hardness by >15 % relative to untreated controls at field strengths ≤1 MV/m. *Falsification criterion:* Hardness reduction <5 % across all tested frequencies at field strengths up to 2 MV/m.

P3 (Component C): Groove signature matching. *Prediction:* SEM and optical profilometry of Petrie core No. 7 will reveal a periodic depth modulation on the helical groove at spatial wavelengths consistent with axial vibration amplitude of a 20–40 kHz oscillating tool (predicted modulation period: 5–50 μm), not present on cores drilled with copper tube plus emery only. *Falsification criterion:* No periodic depth modulation detected at the predicted scale; or modulation consistent with abrasive grain-size variation in a non-vibrating system.

P4 (Component D): Surface microtopography discrimination. *Prediction:* 3D surface scans of joint faces at Sacsayhuamán will show isotropic low-Ra texture characteristic of convergent abrasive lapping, distinguishable from directional hammerstone micro-scar texture at a confidence level >95 % using a pre-specified texture metric (e.g., autocorrelation function isotropy index I_{ac}). *Falsification criterion:* Joint surfaces are statistically indistinguishable from hammerstone-dressed surfaces in I_{ac} and related texture parameters.

P5 (Component E): Boss placement and modal analysis correlation. *Prediction:* The positions of bosses on a minimum of 30 documented Egyptian Old Kingdom ashlars will correlate more strongly with antinodal positions predicted by FEA modal analysis of those block geometries than with positions predicted by lever-mechanics models (measured by mean normalised distance to nearest predicted optimal position, with bootstrapped confidence intervals). *Falsification criterion:* Lever-mechanics positions are a significantly better predictor of boss placement than modal antinodal positions.

P6 (Cross-site): Correlated acoustic resonance and construction precision. *Prediction:* Across a sample of >10 megalithic enclosures spanning Egypt, Malta, and Peru, the presence or absence of interior chamber acoustic resonances in the 40–130 Hz band will correlate positively with the presence or absence of anomalously tight joint tolerances (<0.5 mm gap), controlling for site age and primary stone type. *Falsification criterion:* No significant correlation; or correlation in the predicted direction with $p > 0.05$ in a pre-registered analysis.

8. Proposed Validation Programme

The following experimental programme is designed to generate decisive evidence for or against each component of the framework within a 24-month horizon, assuming access to a university rock-mechanics laboratory, a precision manufacturing facility, and institutional access to the relevant archaeological specimens and sites.

Phase 1 (Months 1–3): Pre-registration and Baseline

Pre-register all six predictions above on the Open Science Framework with complete analysis specifications, outcome metrics, sample sizes, and decision criteria.

Conduct baseline tribometer measurements of stone–soil, stone–timber, and stone–stone friction coefficients without vibration, establishing the μ_0 values that P1 predictions reference.

Phase 2 (Months 2–8): Laboratory Physics Tests

- **P1 test:** Tribometer study with granite, limestone, and andesite samples on compacted earth and timber substrates. Test at 20, 30, and 40 kHz; amplitudes 2, 5, 10, 20 μm; normal loads 50, 200, 500 kN. $n \geq 30$ runs per condition ($3 \times 3 \times 3 \times 4 = 108$ cells, 30 runs each = 3240 tribometer runs; pilot of 20 runs per condition to estimate variance, then adaptive power analysis).
- **P2 test:** Procure Aswan granite samples; replicate Vesterinen et al. (2024) protocol; map hardness as function of frequency, field strength, and fabric orientation. $n \geq 15$ specimens per condition.

Phase 3 (Months 4–12): Drilling and Surface Replication

- **P3 test:** Non-destructive SEM and optical profilometry of Petrie core No. 7 (Petrie Museum, UCL, catalogue reference UC16036) and 4–6 comparable cores. Controlled drilling experiment: copper tube + emery, copper tube + emery + ultrasonic vibration, RUM diamond tool. $n \geq 30$ drilled cores per condition. Groove signature analysis by blinded rater.
- **P4 test:** Field survey at Sacsayhuamán: 3D scan (≤5 μm resolution) of ≥20 joint-face pairs. Laboratory reference surfaces produced by hammerstone dressing, abrasive lapping (no vibration), vibrational lapping. Blinded texture classification.

Phase 4 (Months 8–18): Archaeological Data Collection

- **P5 test:** Photogrammetric documentation of ≥30 bossed ashlars at Giza and associated Old Kingdom sites. FEA modal analysis for each documented block geometry. Statistical comparison of boss positions vs. lever-model and modal-map predictions.
- **P6 test:** Acoustic measurements of ≥10 megalithic enclosures. Joint-tolerance measurements or literature extraction for the same sites. Pre-registered regression.

Phase 5 (Months 18–24): Integration and Publication

Cross-component synthesis: test whether components supported by Phase 2–4 jointly explain the anomaly set better than conventional models (using formal model comparison, e.g., AIC, BIC, or Bayes factor where applicable). Draft peer-reviewed papers for each component; make all data, code, and SEM images open-access.

9. Discussion: Limitations and the Inference Bridge

The most serious limitation of the Resonance Architecture hypothesis, as currently stated, is the *inference bridge*: the gap between well-documented modern laboratory effects and the claim that ancient peoples had systematic access to the equivalent physical conditions. This gap has several sub-problems.

The power source problem. Ultrasonic vibration at useful amplitudes requires energy input at the relevant frequency. Modern implementations use piezoelectric transducers driven by electronic amplifiers. Ancient analogues are not immediately apparent. The framework is deliberately agnostic about the specific implementation, noting that organised rhythmic percussion, natural acoustic resonance amplification in enclosures, and the mechanical coupling of large-amplitude low-frequency oscillations (achievable by coordinated human activity) are all plausible candidates for investigation—but none has been demonstrated experimentally at the required scale and frequency.

This agnosticism is epistemically honest but scientifically unsatisfying. A stronger version of the hypothesis would specify a plausible ancient energy source and demonstrate its adequacy. This is identified as the highest-priority open problem for the framework's long-term viability.

The archaeological silence problem. If vibration-coupled devices were in systematic use, they should have left material traces: specific wear marks on stone tool sockets, residue of coupling media (water, oil), possible wooden or metal components of resonating structures. None of these has been specifically identified. The framework predicts they exist and have either not been looked for (because the hypothesis was not formulated) or have been misidentified. Boss micro-wear analysis (P5) is designed to address this directly.

The scale and logistics problem. Laboratory demonstration of vibration-assisted friction reduction at tribometer scale (contact area $\sim$cm^2, loads $\sim$kN) does not guarantee equivalent behaviour at multi-tonne block scale (contact area $\sim$m^2, loads $\sim$MN). Non-linearities in wave propagation, damping by irregular stone surfaces, and distributed loading may substantially reduce the benefit at scale. Prediction P1 must be tested at progressively larger scales to address this.

Relationship to conventional models. The framework's most productive role may not be as an alternative to conventional models but as a source of new testable predictions that conventional models do not generate. Even if vibrational mechanisms turn out to have played a minor role, the systematic investigation they motivate—groove signature analysis, surface microtopography comparison, modal analysis of bossed ashlars, acoustic cross-site correlation—will produce new data about ancient stoneworking regardless of which model the data ultimately supports.

10. Conclusion

The Resonance Architecture hypothesis is not a claim that ancient peoples possessed modern technology. It is a claim that certain physical phenomena—well-documented in the modern experimental literature on tribology, rock mechanics, and ultrasonic machining—may have been exploited, deliberately or empirically, by ancient craftspeople in ways that explain a set of anomalous observations in the archaeological record. The physics is sound. The archaeological bridge requires building.

The framework's value lies in its dual contribution: it offers a *unified* mechanism family connecting diverse anomalies that conventional models treat independently, and it generates a set of *specific, falsifiable predictions* that are testable with currently available instrumentation and access. Six such predictions have been formalised in §7, and a structured 24-month validation programme has been proposed in §8.

We invite criticism, collaboration, and counter-proposals. The framework stands or falls on experimental evidence, and identifying the evidence that would falsify it is as important as identifying the evidence that supports it. The goal is not to defend a theory but to answer a genuine empirical question: *did vibration play a systematic role in ancient megalithic stoneworking?* Resonance Architecture provides one structured approach to finding out.

References

Bogner, J. (2025). *Resonance Architecture: The Acoustic Technology of the Age of Leo*. Unpublished framework document, December 2025.

Bordes, A., & Volarovich, M. P. (1956). Piezoelectric effect in rocks. *Tectonophysics*, early volume.

Devereux, P. (2014). Ears and Years: Aspects of Acoustics and Intentionality in Antiquity. In C. Scarre & G. Graeme (Eds.), *Archaeoacoustics: The Archaeology of Sound*. Malta: OTS Foundation.

Fernando, P. K. S. C., Zhang, M., & Pei, Z. J. (2018). Rotary ultrasonic machining of rocks: An experimental investigation. *Advances in Mechanical Engineering*, **10**(3), 1–9. https://doi.org/10.1177/1687814018763178

Fox-Rabinovich, G. S., & Totten, G. E. (Eds.) (2006). *Self-Organization During Friction: Advanced Surface-Engineered Materials and Systems Design*. Boca Raton: CRC Press.

Ghomshei, M. M., & Templeton, D. C. (1989). Piezoelectric and α-β quartz transition in a granite: possible implication for rock bursts. *Tectonophysics*, **159**(3–4), 307–313.

Jahn, R. G., Devereux, P., & Ibison, M. (1996). Acoustical resonances of assorted ancient structures. *Journal of the Acoustical Society of America*, **99**(2), 649–658.

Jiao, G. Y., Hu, S., Xu, L., et al. (2021). Review on rotary ultrasonic machining of brittle materials. *International Journal of Advanced Manufacturing Technology*.

Lauro, S., et al. (2025). The friction reduction and stick–slip inhibition effects of ultrasonic vibration on sliding friction pair under solid lubrication. *Tribology Letters*, **73**. https://doi.org/10.1007/s11249-025-01969-2

Lauro, S. E., et al. (2023). The inhibition mechanism of ultrasonic vibration on the stick-slip phenomenon. *Scientific Reports / Nature*.

Lehner, M. (1997). *The Complete Pyramids*. London: Thames & Hudson.

Marinescu, I. D., Rowe, W. B., Dimitrov, B., & Ohmori, H. (2012). *Tribology of Abrasive Machining Processes* (2nd ed.). Oxford: William Andrew/Elsevier.

Nosonovsky, M., & Bhushan, B. (2009). Thermodynamics of surface degradation, self-organization and self-healing for biomimetic surfaces. *Philosophical Transactions of the Royal Society A*, **367**, 1607–1627.

Petrie, W. M. F. (1883). *The Pyramids and Temples of Gizeh*. London: Field & Tuer.

Popov, V. L., & Gray, J. A. T. (2012). Prandtl–Tomlinson model: history and applications in friction, plasticity, and nanotechnologies. *ZAMM — Journal of Applied Mathematics and Mechanics*, **92**(9), 683–708.

Protzen, J.-P. (1986). Inca stonemasonry. *Scientific American*, **254**(2), 94–105.

Reznikoff, I. (2014). On the Sound Related to Painted Caves and Rocks. In A. Rubin et al. (Eds.), *Archaeoacoustics: The Archaeology of Sound*. Malta: OTS Foundation.

Saarenrinne, M., et al. (2023). Weakening of compressive strength of granite by piezoelectric actuation of quartz using high-frequency and high-voltage alternating current: A 3D numerical study. *Rock Mechanics and Rock Engineering*, **56**. https://doi.org/10.1007/s00603-023-03451-8

Stocks, D. A. (2023). *Experiments in Egyptian Archaeology: Stoneworking Technology in Ancient Egypt* (2nd ed.). London & New York: Routledge.

Storck, H., Littmann, W., Wallaschek, J., & Mracek, M. (2002). The effect of friction reduction in presence of ultrasonic vibrations and its relevance to travelling wave ultrasonic motors. *Ultrasonics*, **40**(1–8), 379–383.

Vesterinen, V., et al. (2024). Progressive weakening of granite by piezoelectric excitation of quartz with alternating current. *Rock Mechanics and Rock Engineering*, **57**, 7963–7973. https://doi.org/10.1007/s00603-024-03948-w